Suzaku/XIS Observations of 1E 0102-72.3

E. Miller (MIT/Osaka U.), **M. Tsujimoto** (Rikkyo, target leader), **A. Bamba** (RIKEN),
T. Dotani (ISAS/JAXA), **K. Hayashida** (Osaka U.), **J. Hiraga** (ISAS/JAXA), **S. Kitamoto** (Rikkyo),
B. LaMarr (MIT), **A. Sekiguchi** (Rikkyo)

INTRODUCTION & OBSERVATIONS

1E 0102-72.3 (hereafter E0102) is a bright, oxygen-rich SNR in the SMC. The X-ray spectrum is dominated by low-energy line emission, making the source a popular X-ray mission calibration target for tracking changes in low-energy gain and effective area. Here we present five observations of E0102 by the XIS onboard *Suzaku*, with a focus on characterizing changes in the low-energy effective area likely due to OBF contamination buildup. We also compare the best-fit model with one from the literature.

The observations are summarized in Table 1. The rev0.6 processed data were filtered based on the light curve, and residual hot pixels were removed. The SNR X-ray emission is spatially unresolved by the XIS; Chandra imaging shows a ring of X-ray emission, 14" in diameter, closely associated with radio and optical line emission (see Figure 1). We extracted the spectra using a 6mm source region centered on the chip, and an annulus for the background (see Figure 2).

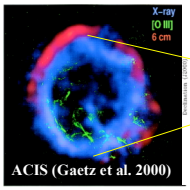

Figure 1

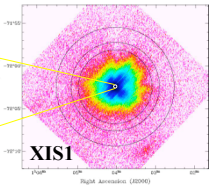

Figure 2

TABLE 1. OBSERVATIONS

date	ksec	notes
2005 Aug 13	3	XIS door open
2005 Aug 31	24	…
2005 Dec 16	63	111 ksec for XIS1
2006 Jan 17	9	SW update
2006 Feb 02	21	…

MODELING

We adopted a model based on *Chandra* and *XMM-Newton* grating observations (Flanagan et al. 2004, Rasmussen et al. 2001). The model, kindly provided by P. Plucinsky (CXC/CfA), is composed of 24 Gaussian emission lines below 2 keV superposed on a bremsstrahlung continuum, with separate absorption components from the SMC and the Galaxy. An example spectrum with the lines identified is shown in Figure 3.

Our strategy to characterize the effective area degradation was as follows. The contamination-free model was fit to the three FI spectra from 2005-08-13, an observation performed immediately after the XIS doors were opened. The BI data were excluded due to the warmer (-80°C vs. -90°C) CCD operating temperature at this time. The line and continuum normalizations were allowed to vary freely. Line centers, *kT*, and the Galactic absorption column were fixed at expected values. To account for inaccuracies in the spectral resolution, we included a single free parameter for the line width for each detector. Finally, we varied the SMC absorption column within the expected (broad) range, fitting three separate models for $N_{H,SMC}$ = 0, 2, and 5×10^{20} cm^{-2}. The model parameters for the best fit model ($N_{H,SMC}$ = 2×10^{20} cm^{-2}) are shown in Table 2, along with a comparison to *Chandra*/HETG measurements (Flanagan et al. 2004). Our absorption-corrected line fluxes agree to about 30%.

These models were used to determine the extent of the contamination. We fit the five epochs for each detector assuming pure carbon absorption, freezing the line and continuum normalizations. Once again a single line width and gain fit parameters were allowed to vary.

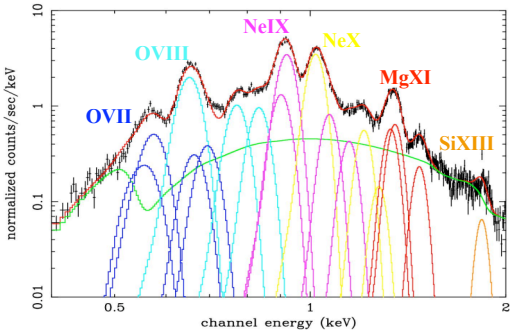

Figure 3. XIS1 (BI) spectrum of E0102. Emission lines are color-coded to the responsible species. The bremsstrahlung emission is shown in green.

TABLE 2. E0102 MODEL $\chi^2 = 1.15$ (416 dof)

contamination (varabs)	C only, varies by detector, epoch
Galactic absorption (vphabs)	$N_H = 5.36\times10^{20}$ cm^{-2}, solar abund
SMC absorption (phabs)	N_H = 0, 2, and 5×10^{20} cm^{-2}, SMC abund
continuum (bremss)	kT = 0.74

E0102 EMISSION LINE FLUX

species	transition	energy (keV)	XIS flux	HETG flux[a]	ratio[b]
			10^{-4} photons s^{-1} cm^{-2}		
OVII	forbidden	0.561	25.0±0.2	18.5±2.9	1.4±0.2
OVII	resonance+intercomb	0.574	43.2±0.2	33.5±4.9	1.3±0.2
OVIII	Lyα	0.654	52.7±0.3	49.4±9.0	1.1±0.2
OVII	Kβ	0.665	7.2±0.3	6.7±1.4	1.1±0.3
OVII	Kγ	0.698	6.7±0.2	2.3±1.4	2.9±0.8
OVIII	Lyβ	0.774	10.9±0.1	6.5±1.2	1.7±0.2
OVIII	Lyγ	0.817	7.3±0.1	4.6±0.4	1.6±0.2
NeIX	forbidden	0.905	7.9±0.3	8.6±1.2	0.9±0.2
NeIX	resonance+intercomb	0.923	19.4±0.4	16.2±1.4	1.2±0.1
NeX	Lyα	1.022	15.1±0.1	11.2±0.9	1.3±0.1
NeIX	Kβ	1.073	3.2±0.1	3.5±0.2	0.9±0.1
NeIX	Kγ	1.127	1.5±0.2	2.2±0.4	0.7±0.1
NeX	Lyβ	1.212	1.8±0.2	2.3±0.3	0.8±0.1
NeX	Lyγ	1.277	0.4±0.1	…	…
MgXI	forbidden	1.331	1.7±0.1	…	…
MgXI	resonance+intercomb	1.352	1.9±0.2	4.1±0.3	0.5±0.1
MgXII	Lyα	1.473	0.6±0.1	1.1±0.1	0.6±0.1
SiXIII	triplet	1.840	0.2±0.1	1.1±0.2	0.2±0.1

a - *Chandra*/HETG observed line flux (Flanagan et al. 2004), corrected for our fit absorption
b - XIS line flux divided by HETG line flux

CONTAMINATION RATE

The best fit carbon absorption column varies by detector and as a function of time, as can be seen in the spectra and the history plot (Figures 4 and 5). XIS3 exhibits the strongest absorption, and the contamination rate is well-described by a straight line for the first four observations. The rates for XIS2 and XIS3 appear to turn over in the latest observation. Interestingly, the sensor bases for these two detectors have been 5-10 °C warmer during the last two observations than the previous observations. It is unclear at this point whether a deposition/evaporation equilibrium has been reached.

The systematic error indicated in Figure 5 is determined by fitting with different fixed SMC absorption columns. The slope of the fit line does not change, only the intercept offset.

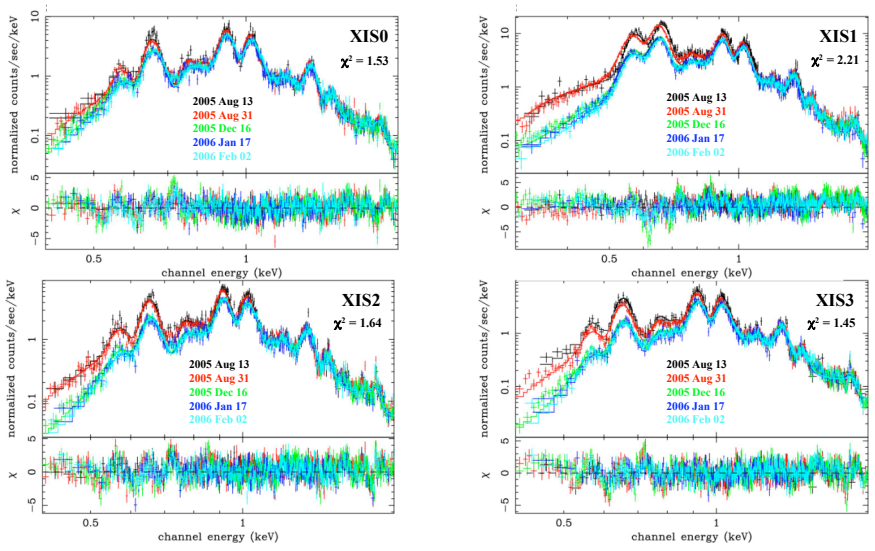

Figure 3. Combined spectra for E0102, showing best fit contamination model for each detector.

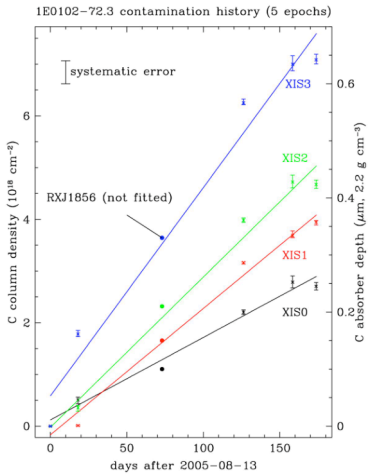

Figure 5. Carbon contamination depth vs. time. Straight lines were fit to the data for each sensor, assuming zero contamination at zero time. XIS3 shows the worst absorption, with a possible turnover at late times.